

Research Journal of Pharmaceutical, Biological and Chemical Sciences

The Effects of N68 Mutation on the Thermal Stability of apo-CP43 via Fluorescence Spectroscopy.

Ji Liu[#], Si-Si Xie[#], Jing-Zhang Wang, Guo-Fei Zhu, Lin-Fang Du^{*}

Key Laboratory of Bio-resources and Eco-environment of the Ministry of Education, College of Life Sciences, Sichuan University, Chengdu 610064, P.R. China

ABSTRACT

CP43 is a chlorophyll binding protein, which is also the internal antenna system of photosystem II located in the thylakoid membrane of plants. To study the functional and structural aspects of apo-CP43 under stresses, we purified it and the N68F mutant in *Escherichia coli*, and investigated the thermal stabilities of them by means of intrinsic tryptophan fluorescence, synchronous fluorescence, and extrinsic ANS fluorescence spectroscopies. The intrinsic tryptophan fluorescence and synchronous fluorescence experiments indicated that heat treatment induced changes in the substructures in apo-CP43 WT and the N68F mutant, resulting in the polarity in the microenvironments of the tryptophan residues increased, and the N68F mutant changed more significantly than the WT. ANS fluorescence measurements also showed that the loss of structure was larger in the N68F mutant than in the WT. The results reveals a reduced thermal stability of the mutated apo-CP43 compared to the WT protein, with the main thermal transition temperatures was 50.8 °C for WT and 36.9 °C for the mutant, respectively. The results suggests that the N68 site mutagenesis decreases the thermostability of the apo-CP43, indicating that the potential binding sites for pigment, N68 may be the key amino acid stabilizing the structure of transmembrane helix in apo-CP43.

Keywords: apo-CP43; Mutagenesis; Thermostability; Fluorescence spectroscopy; Synchronous fluorescence; ANS

* Address for correspondence

These two authors contributed equally to this work.

INTRODUCTION

Photosystem II (PS II) is a large pigment–protein complex located in the thylakoid membrane of plants. It is the light-driven water:plastoquinone oxidoreductase of oxygenic photosynthesis, responsible for producing most of the oxygen in the atmosphere [1]. Crystal structures of dimeric PSII protein complexes isolated from the thermophilic cyanobacteria *Thermosynechococcus elongatus* [2-5] and *Thermosynechococcus vulcanus* [6,7] have revealed the organisation of the 20 subunits within each monomeric complex and the positions of the various co-factors. The outer part of PS II is the light-harvesting chlorophyll (Chl) *a/b* pigment–protein complex (LHCII). At the heart of the complex are the D₁ and D₂ reaction centre (RC) sub-units, where primary charge separation and water oxidation occur. Closely associated with the RC are two similar chlorophyll-binding proteins, CP43 and CP47. The chlorophyll binding proteins CP43 and CP47 are the internal antenna system of photosystem II (PS II). In addition to their roles as proximal antennae proteins for the photosystem, both CP43 and CP47 appear to interact with proteins associated with the site of water oxidation [8-9]. CP43 also involved in ligating the Mn₄Ca cluster [3]. CP43 is encoded by the *psbC* gene while the *psbB* gene encodes CP47. Although their apparent molecular masses, as judged by SDS-PAGE are 43 and 47 kDa, the calculated molecular masses for spinach proteins are 50 and 56 kDa, respectively [8-9]. CP43 has six transmembrane α -helices, which are separated by five extrinsic loop domains, and it contains 473 amino residues. It binds chlorophyll *a* (13 in CP43 and 16 in the CP47) and β -carotene (4 for CP43 and 5 for CP47) [4,10].

Early studies indicated that deletion of the *psbC* gene leads to a loss of photoautotrophic growth and oxygen-evolving capacity [11, 12], and introduction of short deletions in the large extrinsic loop E of C centers capable of transferring electrons from hydroxylamine to Q_A, but can not grow photoautotrophically, exhibits only 10% of the steady-state oxygen evolution rate of wild type when grown photoheterotrophically (< 3% when grown mixotrophically), with this low residual oxygen evolution capacity being very susceptible to photoinactivation [14, 15]. A number of the histidyl residues located in the transmembrane helices of CP43 have also been probed by site-directed mutagenesis to clear if they are the ligand of chlorophyll [16]. CP43 has a profound effect on the assembly of functional PS II core complexes in vivo [13] comparable to that observed upon deletion of the *psbC* gene. C. Putnam Evans' laboratory has introduced a number of point mutations in the large extrinsic loop E of CP43. It is showed that some mutants appear to assemble into functional PS II reaction centers at moderate yields, and fluorescence measurements indicated that the mutants assemble 60–70% of the PS II.

However, there is no study on the expression and purification of the apo-CP43 in *E.coli* BL21 after introducing the point mutation to the transmembrane helices I of apo-CP43 in vitro, and the stability of apo-CP43 has not yet been reported. Nowadays, biomolecular dynamics and stability are investigated both in vitro [17-19] and in the living cell [20]. Thermal stability is essential for the proper functions of a protein, for the stability of the protein may significantly affects its biological functions [21]. In this study, we focused the

research on the thermal stability of the spinach apo-CP43. Briefly, a mutation has been introduced to the position of Asn-68 (N68) and substituted with Phe. Then, we expressed and purified the WT and the mutant apo-CP43 (N68F) in BL21 *E. coli*. With the aim of elucidating the biological characteristics of the WT and N68F mutant, we conducted the experiments focused on the reversibility of the thermal unfolding of the WT and N68F mutant, by means of spectroscopic assay, such as intrinsic tryptophan fluorescence and 8-anilino-1-naphthalenesulfonic acid (ANS) fluorescence. ANS fluorescence is strongly dependent on the hydrophobicity of the environment [22, 23], which can be used to determine the unfolding of hydrophobic clusters in WT and N68F mutant. These researches will also pave the way for the studies of reconstitute of the chlorophyll *a* and the apo-CP43 in vitro.

MATERIALS AND METHODS

Materials

BL21 *E. coli* strains were used for expression and purification of the WT and the N68F mutant. HisTrap HP prepacked with Ni Sepharose High performance was obtained from Amersham. Tris, urea and GdnHCl, SDS, ANS and Isopropyl thio- β -D-galactoside (IPTG) were purchased from Sigma Chemical Company (USA). All other chemicals were local products of analytical grade. Solutions were prepared with Milli-Q water.

Expression and purification of apo-CP43

The gene of WT and N68F were cloned into the PET-28a expression vector, and the recombinant protein was expressed in *E. coli* BL21 [24]. In brief, the recombinant strains were incubated at 37 °C for 12 h in Luria–Bertani medium containing 30 μ g/mL kanamycin. The cultures were diluted (1 : 100) in the same medium and grown at 37 °C to reach an attenuation of approximately 0.6. The expression of the recombinant proteins was induced by 1 M IPTG at 27 °C and the cells were harvested after 4 h of induction. The cells were harvested by centrifugation at 4000 rpm for 10 min at 4 °C. The cells were washed and resuspended in buffer A (20 mM Tris-HCl, 0.5 M NaCl, 5 mM imidazole pH 8.0), and then the cells were lysed by an ultrasonic oscillator. After centrifugation at 10000 rpm for 20 min, the extracted recombinant soluble proteins were purified by Ni-chelating column (HisTrap HP) in the AKTA FPLC system (Amersham Pharmacia Biotech, Uppsala, Sweden). The column was washed using buffer A, and his-apo-CP43 or the mutant were eluted using buffer B (20 mM Tris-HCl, 0.5 M NaCl, 100 mM imidazole pH 8.0). Imidazole was removed by SEC-FPLC using HR 10/30 Superpose 6 column (Pharmacia) on an AKTA FPLC. SDS–PAGE analysis was used to detect the purity of the purified proteins, and the protein concentration was determined according to the Bradford method using bovine serum albumin (BSA) as a standard. The concentration of the stock solution of WT and the mutant in Tris–HCl buffer (pH 7.0) were 10 mM, which were used for intrinsic tryptophan fluorescence and ANS fluorescence spectra.

2.3 Thermal stability of apo-CP43

The thermal stability of WT and N68F mutant were assayed by treated at different temperatures ranging from 20 to 100 °C as described above. Another sample without incubation was set as a control. After the incubation, the solutions were cooled on the ice and then centrifuged at 12, 000 rpm for 10 min. The relative amounts of the apo-CP43 in these supernatants were estimated quantitatively from the absorption of the protein.

Measurements of the fluorescence spectra

Fluorescence spectra were performed in a quartz cuvet with 1 cm path length on a Hitachi F-4500 fluorescence spectrophotometer equipped with a circulating water bath. Excitation slit and emission slit were set as 5 nm. The samples were secured at each temperature from 25 to 95 °C for 10 min before the fluorescence spectra were recorded. The fluorescence emission spectrum of each heat-treated sample was recorded between 310 and 400 nm with $\lambda_{\text{ex}} = 295$ nm in 20 mM Tris-HCl (pH 7.0) at 25 °C. The synchronous fluorescence spectra were recorded between 270 and 320 nm when $\Delta\lambda = 15$ nm, and were recorded between 250 and 300 nm when $\Delta\lambda = 60$ nm, where $\Delta\lambda$ is a constant wavelength interval, $\Delta\lambda = \lambda_{\text{em}} - \lambda_{\text{ex}}$ [25]. Background intensity in the samples without protein was always subtracted and the fluorescence spectra were corrected.

Calculate the fraction of unfolded WT and the mutant apo-CP43

The fluorescence intensity at each temperature was normalized by deducting the disturbance from the thermal quenching [26]. The fraction of unfolded WT and the N68F mutant at each temperature was calculated using the following equation [27]:

$$F_D = (F_t - F_0) / (F_d - F_0) \quad \text{Eq. (1)}$$

where F_D is the amount of denatured WT or the N68F mutant at a temperature, F_t is the fluorescence intensity at the temperature, F_0 and F_d are the fluorescence intensities in the native and denatured states, respectively.

T_m , the temperature at which 50% of apo-CP43 was unfolded, can be calculated from the plotting of F_D against temperature.

Measurements of the ANS fluorescence spectra

ANS is an extrinsic fluorescence probe that binds to the hydrophobic patches present on a protein surface. Hence, protein-bound ANS fluorescence represents the surface hydrophobic properties of a protein molecule [28]. Apo-CP43 bound ANS fluorescence is the fluorescence intensity of the ANS-apo-CP43 conjugate minus that of ANS alone. The samples of WT and N68F (5 mL) were diluted by 20 mM Tris-HCl buffer (pH 7.0) and were secured at each temperature from 25 to 95 °C for 10 min, then ANS (5 mM) was add to get a mixture of 0.5 μM protein and 10 μM ANS in 20 mM Tris-HCl (pH 7.0). The spectra were recorded on a Hitachi F-4500 fluorescence spectrophotometer, and excitation slit and emission slit were set

as 5 nm. The ANS fluorescence was measured in the range of 400 - 600 nm with $\lambda_{ex} = 380$ nm after the samples had been incubated for 1 h in the dark.

RESULTS AND DISCUSSION

Thermal stability of WT and the N68F mutant of apo-CP43

The thermal stabilities of WT and the N68F mutant were analyzed by monitoring the amounts of the proteins in the supernatants after they were incubated at increasing temperatures for 10 min. After centrifugation, the supernatants were collected and the amounts of them were measured by the Bradford method. Fig. 1 showed that the amounts of WT decreased gradually above 40 °C, but the N68F mutant decreased dramatically. Nearly 40% lost of WT was observed at 100 °C, while the N68F mutant lost almost all at last, so we can conclude that WT had a relatively high thermal stability than the N68F mutant. The result also indicated the unfolding of the hydrophobic groups in the proteins, which aggregated and resulted in the protein precipitation with the increasing temperature.

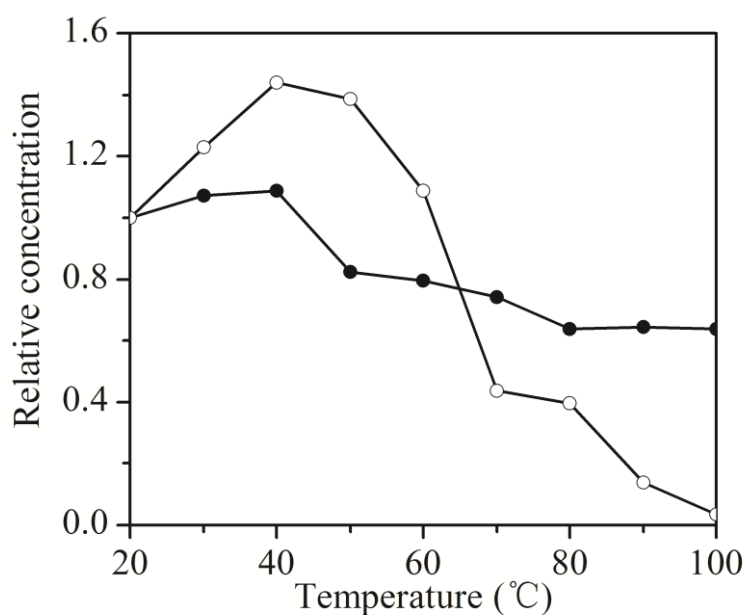


Fig. 1. Thermal stability of the WT (●) and the N68F mutant (○) of apo-CP43, as revealed by the relative amounts in the supernatants after the incubations from 25 to 95 °C for 10 min.

Temperature induced conformational transition in WT and the N68F mutant of apo-CP43 as revealed by intrinsic fluorescence

Thermal denaturation involves possible destruction of both the secondary and the tertiary structures, and may make a protein unfold and expose the side chains of the hydrophobic residues embedded inside native structure. Then, the thermal denaturation of a protein can be obtained by monitoring the exposure of hydrophobic residues [29]. The native apo-CP43 contains several fluorescence reporter groups, such as five tryptophan

residues and three tyrosine residues in transmembrane helices, and five tryptophan residues and one tyrosine residues in extrinsic loop [9]. As an indicator of structural changes, the intrinsic fluorescence spectra of WT and the N68F mutant were monitored, which are sensitive to the tertiary structure and the conformational stability of protein in solution. Fig. 2 showed that the fluorescence emission spectra of WT and the N68F mutant with the increasing temperature when $\lambda_{\text{ex}} = 295 \text{ nm}$. At 25 °C, the fluorescence intensity was highest, and the λ_{max} of the WT and the N68F was located at 336.8 nm and 340 nm, respectively. It suggests that the tryptophan residues were located in relatively hydrophobic environments in the proteins [33]. From 25 °C to 60 °C, the λ_{max} of the spectra changed only a little, but significant red shift was observed at higher temperature. At 95°C, the λ_{max} was located at 347.8 nm and 351.4 nm, respectively, primarily indicating that the polarity around the tryptophan residues in WT and the N68F mutant was increased. These results also showed that the hydrophobic environments around the tryptophan residues of the two proteins have some differences, which will be shown in details in the next.

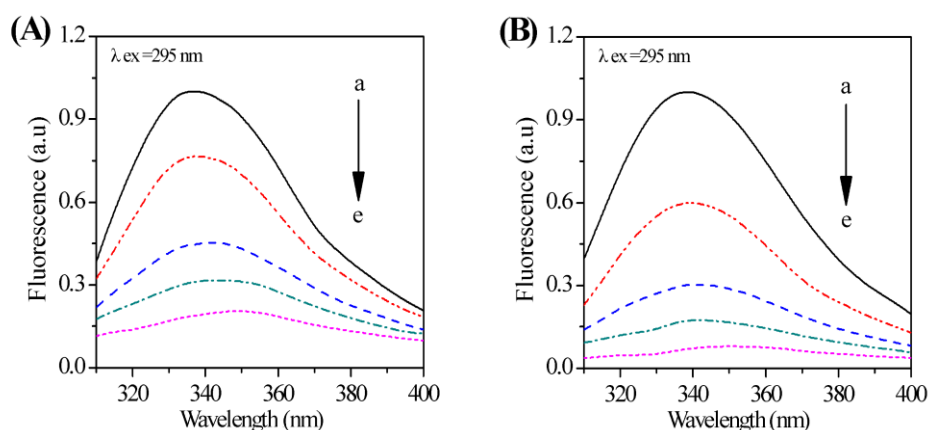


Fig. 2. Fluorescence emission spectra of the WT (A) and the N68F mutant (B) form of apo-CP43 with increasing temperature when $\lambda_{\text{ex}} = 295 \text{ nm}$. a→e: 25, 40, 60, 80 and 95°C, respectively.

The synchronous fluorescence spectra present the characteristic information of the tyrosine residues or the tryptophan residues, when the D-value between excitation and emission wavelength is stabilized at 15 or 60 nm, respectively [25]. Fig. 3 represented the synchronous fluorescence spectra of WT and the N68F mutant with the increasing temperature. The λ_{max} of WT was located at 286.2 nm at 25 °C when $\Delta\lambda = 15 \text{ nm}$, and it was located at 285.4 nm for the mutant. The λ_{max} of the spectra blue shifted with the increasing temperature, from 286.2 to 282 nm and from 285.4 to 281.8 nm for WT and the N68F mutant, respectively, indicating that the polarity around the tyrosine residues in the two proteins decreased and the hydrophobicity increased [30]. Correspondingly, the λ_{max} for WT and the N68F mutant was located at 278.8 nm and 279 nm at 25 °C when $\Delta\lambda = 60 \text{ nm}$, respectively. And slight red shifts (from 278.8 to 280.8 nm and from 279 to 281 nm for WT and the N68F mutant, respectively) were observed from 25 to 95 °C, indicating that heat treatment loosen structure of the proteins, and affect the microenvironment of the tryptophan residues [31]. It was also showed that the maximum fluorescence intensity of the N68F mutant decreased obviously with the increasing temperature.

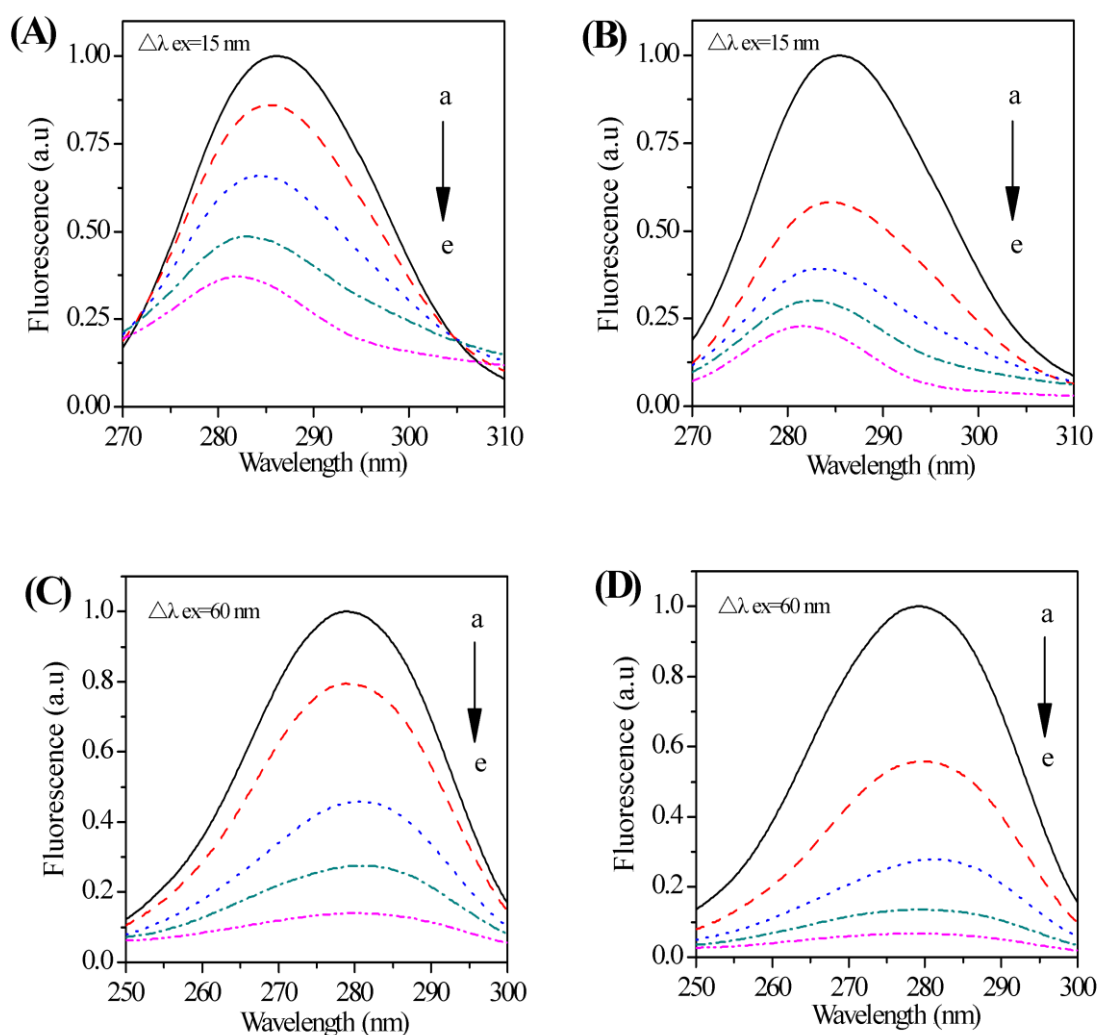


Fig. 3. Synchronous fluorescence spectra of the WT (A and C) or the N68F mutant (B and D) form of apo-CP43 with increasing temperature when $\Delta\lambda = 15$ nm and 60 nm. a \rightarrow e: 25, 40, 60, 80 and 95 °C, respectively.

In order to intensively investigate the changes in the microenvironments of the tryptophan and tyrosine residues of the WT and the N68F mutant, the F_{355}/F_{330} ratio (Fig. 4A) and the F_{295}/F_{280} ratio (Fig. 4B) were used to monitor the shifts in the λ_{\max} of the fluorescence emission spectra ($\lambda_{\text{ex}} = 295$ nm) and the synchronous fluorescence spectra ($\Delta\lambda = 15$ nm), respectively [32]. In Fig. 4A, the changes in the F_{355}/F_{330} ratios of the two proteins were very small from 20 to 45 °C. The ratios increased gradually from 45 to 65 °C, and then increased much sharply from 70 to 95 °C, indicating the transferring of the Trp residues to an environment much more polar than in their native conformations [33]. While the F_{355}/F_{330} ratios of the N68F mutant increased more dramatically than the WT when the temperature was above 75 °C, showing that the polarity in the microenvironments of the tryptophan residues in the N68F mutant increased significantly. Compared to the shifts in λ_{\max} of the fluorescence spectra of the tryptophan residues, the changes in the synchronous fluorescence spectra ($\Delta\lambda = 15$ nm) of the tyrosine residues was very different, shown in Fig.

4B. At first, the F_{295}/F_{280} ratios of the WT decreased slowly from 25 to 80 °C, for the N68F mutant, the ratios decreased slowly from 25 to 70 °C, then the ratios of the two proteins decreased significantly until 95 °C, and the N68F mutant decreased more obviously, suggesting that the hydrophobicity around the tyrosine residues of the two proteins increased and the polarity around them decreased [34], and the N68F mutant changed more significantly.

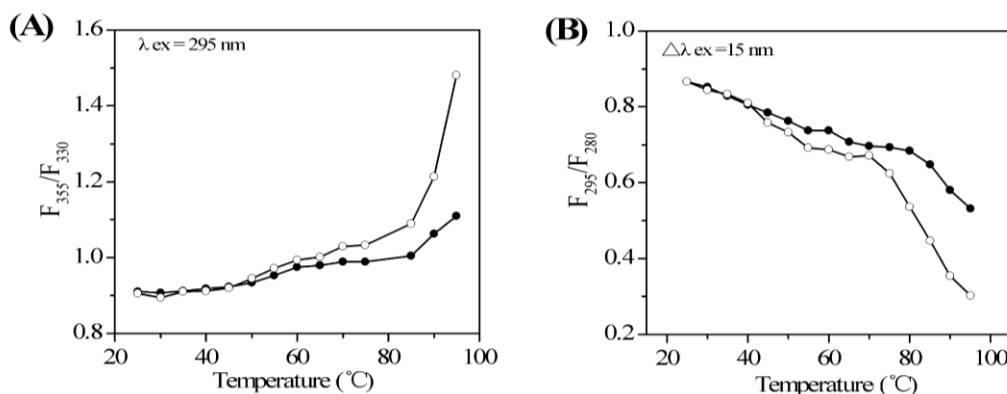


Fig. 4. Temperature induced shifts in λ_{max} of the fluorescence emission spectra of the WT (●) and the N68F mutant (○) form of apo-CP43. (A) Shifts in λ_{max} of the fluorescence emission spectra when $\lambda_{ex} = 295 \text{ nm}$, monitored by the F_{335}/F_{330} ratios. (B) Shifts in λ_{max} of the synchronous fluorescence spectra when $\Delta\lambda = 15 \text{ nm}$, monitored by the F_{295}/F_{280} ratios.

Fig. 5 showed the detailed changes in the maximum fluorescence intensity of the WT and the N68F mutant, monitored by fluorescence emission spectra ($\lambda_{ex} = 295 \text{ nm}$) and the synchronous fluorescence spectra ($\Delta\lambda = 15 \text{ nm}$), respectively. In Fig. 5A, the changes in the maximum fluorescence intensity of the WT decreased gradually from 25 to 60 °C, and then decreased more slowly when the temperature was above 60 °C. For the N68F mutant, the changes in the maximum fluorescence intensity decreased significantly from 25 to 95 °C. Fig. 5B showed that in the synchronous fluorescence spectra ($\Delta\lambda = 15 \text{ nm}$), the maximum fluorescence intensity of the two proteins had a similar trend compared with the changes in fluorescence emission spectra ($\lambda_{ex} = 295 \text{ nm}$).

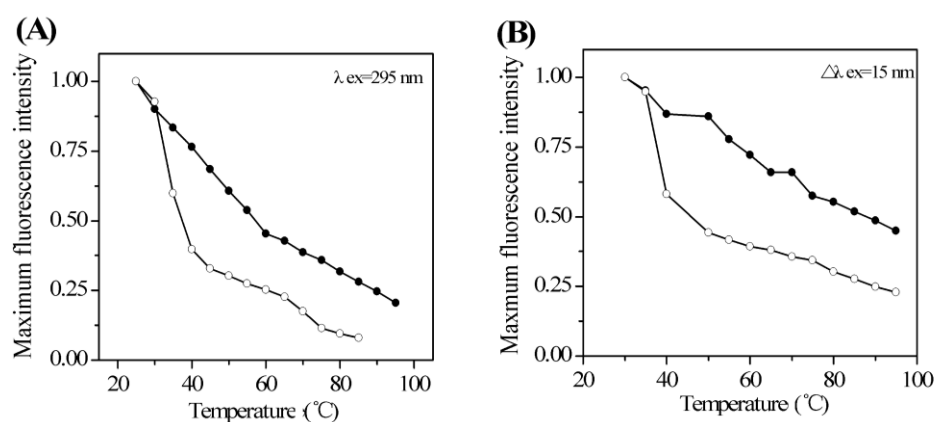


Fig. 5. Temperature induced shifts in the WT (●) and the N68F mutant (○) form of apo-CP43, monitored by (A) the maximum fluorescence intensity of intrinsic fluorescence spectra when $\lambda_{ex} = 295 \text{ nm}$, (B) the maximum fluorescence intensity of synchronous fluorescence spectra when $\Delta\lambda = 15 \text{ nm}$ after heat treatment.

More importantly, based on the fluorescence intensities of the tryptophan and tyrosine residues, we calculated the fraction of unfolded WT and the N68F mutant using Eq. (1), and plotted the normalized data in Fig. 6A and B, respectively. Both WT and the N68F mutant gradually unfolded with the increasing temperature. For the unfolding process monitored by the tryptophan fluorescence (Fig. 6A), the T_m of WT was 50.8 °C in the range of 25-95 °C, and for the N68F mutant was 36.3 °C. For the unfolding process monitored by tyrosine fluorescence (Fig. 6B), the T_m of the WT and the N68F mutant were 61.9 °C and 42.1 °C in the range of 25-95 °C, respectively. The T_m of the N68F mutant always lowers than WT, indicating that the thermal stability of the N68F mutant is inferior to WT.

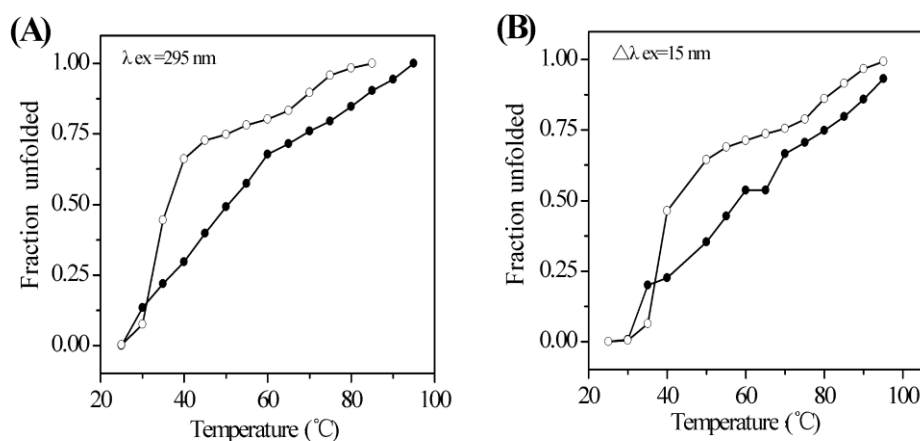


Fig. 6. Fraction of unfolded WT (●) and the N68F mutant (○) form of apo-CP43 monitored by the changes in fluorescence intensity. (A) Fraction of unfolded WT and the N68F mutant of apo-CP43 calculated based on the fluorescence emission intensity at $\lambda_{ex} = 295$ nm and $\lambda_{em} = 350$ nm after heat treatment. (B) Fraction of unfolded WT and the N68F mutant of apo-CP43 calculated based on the synchronous fluorescence intensity when $\Delta\lambda = 15$ nm and $\lambda_{em} = 290$ nm after heat treatment.

Previous studies showed that the denaturation of LHCII began at 65 °C [35] and the main thermal transition of RC was 42 °C [36]. The CP43 purified from spinach occurred at 50 °C [37] to 59 °C [36], while our data indicates that the T_m of WT apo-CP43 and the N68F mutant were 50.8 °C and 36.3 °C. The thermal transition of the WT apo-CP43 (50.8 °C) is similar to the CP43 isolated from spinach (50 °C), primarily indicating that apo-CP43 already has enough folding and stability, and its stability dose not change obviously after pigment binding to it. That is to say even if the pigment dose not bind to the apo-CP43, it may already be very close to the natural conformation, which will pave the way for the studies of reconstitute of the chlorophyll a and the apo-CP43 in vitro. However, for the N68F mutant, the structure is more vulnerable to be broken with the increasing temperature, and it may be anticipated that the N68F mutant has substantially more hydrophobic surface than WT. Other studies on the CP43 isolated from spinach using other techniques (such as circular dichroism (CD) spectroscopy and Fourier transform-infrared spectroscopy and so on) showed that the thermal denaturation process of CP43 can be divided into several phases, upon heat treatment the aggregation, degradation and the secondary structure changes are not simultaneous but follow different courses [8, 38]. In this study, based on the results

above, we tentatively speculate that the hydrophobic of soluble aggregation of apo-CP43 occurred firstly upon heat treatment, and the structure of the denatured proteins changed by high temperatures, as a result, the denatured apo-CP43 aggregates.

The results above indicated that high temperature treatment disrupted the substructures around both of the tryptophan and tyrosine residues in WT and the N68F mutant, but the changes in the polarity and hydrophobicity around them were different from each other. The N68F mutant changed more significantly than WT, indicating that N68 is very important to the structural stability of apo-CP43.

Temperature induced conformational transition in WT and the N68F mutant of apo-CP43 revealed by ANS fluorescence

The tryptophan fluorescence are only symptomatic of local changes in the tryptophan environment, so we suggest that more methods should be carried out to make a systematic investigation of the thermal unfolding of apo-CP43. ANS is a much-utilized fluorescent “hydrophobic probe” for examining the non-polar characteristic of a protein [39]. It is generally assumed that if ANS becomes brilliantly fluorescence upon binding a host protein, the binding sites were non-polar and hydrophobic during association. Despite the fact that ANS is routinely used as a reagent for determining the non-polar surface properties of protein molecules, almost no studies on the unfolding process of the apo-CP43 have been carried out over the years. In this paper, ANS fluorescence spectroscopy is used to study the unfolding of the hydrophobic clusters in WT and the N68F mutant. The fluorescence of free ANS is very weak in aqueous solution. However, once binding to hydrophobic clusters in a protein, the fluorescence intensity of ANS increases significantly, and λ_{\max} of the spectra blue shifts [27, 40].

After treatment from 25 to 95 °C, the detailed changes in the maximum emission wavelength showed in Fig. 7A, and the fluorescence intensity of ANS fluorescence are plotted in Fig. 7B. Interestingly, compared to the theories mentioned above, the situation to the maximum emission wavelength and fluorescence intensity of ANS fluorescence of WT and the N68F mutant was basically reversed. After heating from 30 to 90 °C, the λ_{\max} of WT red shifted from 510 to 516 nm, and the fluorescence intensity decreased by 44.4%. For the N68F mutant, the λ_{\max} of the spectra red shifted from 500.5 to 513.5 nm, and the fluorescence intensity decreased by 56% with the temperature ranging from 30 to 80 °C. These results indicated that maybe both the WT and N68F mutant almost are not susceptible to bind to ANS after heat treatment. It is reported that CP43 possess six transmembrane α helices, and these helices were separated by five extrinsic loop domains (designated extrinsic loops A–E) [8-9]. Maybe the extrinsic loops is the main ANS-binding sites, aggregation and structure changes occurred with temperature increasing, resulting in the decrease of ANS fluorescence intensity and the gradually red-shifted of ANS fluorescence. Compared to WT, the ANS fluorescence of the N68F mutant changed more obviously as similar as the results observed in the intrinsic and synchronous fluorescence.

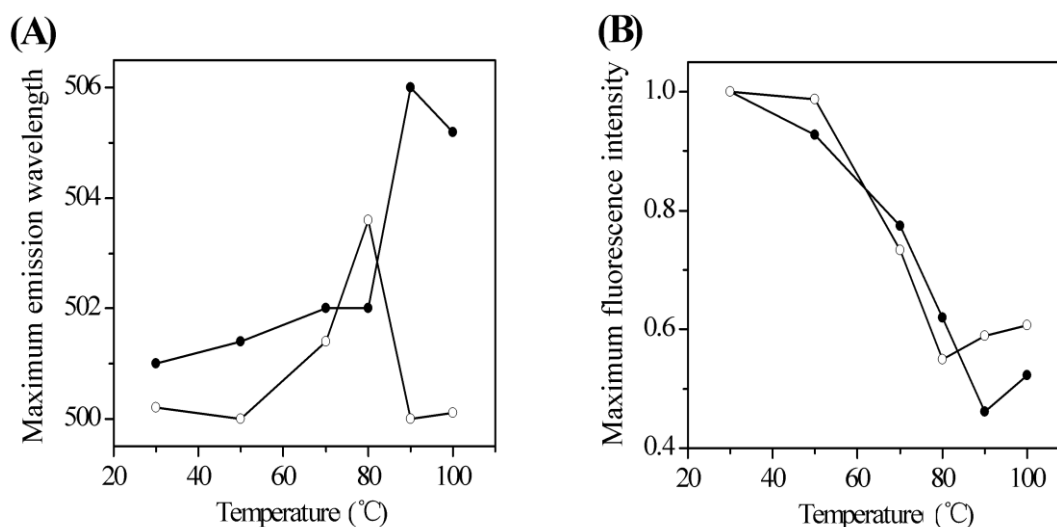


Fig. 7. Temperature induced unfolding of the hydrophobic clusters in the WT (●) and the N68F mutant (○) of apo-CP43, as revealed by ANS fluorescence spectroscopy ($\lambda_{\text{ex}} = 380 \text{ nm}$). (A) Maximum emission wavelength; (B) maximum fluorescence intensity of the ANS fluorescence spectra after heat treatment.

CONCLUSION

Previous studies mainly used "functional probe" absorption spectra of the red region and visible spectra of red region CD, and "structural probe" far-ultraviolet CD to research the CP43 purified from plant [8-9, 37]. In our study, we mainly used "structural probe" fluorescence to investigate the thermostability of the apo-CP43 expressed from *E.coli* BL21. The results presented in this paper have shown that the introduction of a point mutation at the position N68 in apo-CP43 reduces the thermostability of the native protein. The substructures around both of the tryptophan and tyrosine residues in WT and the N68F mutant were disrupted when the temperature was above 50.8 °C and 36.9 °C, respectively. As can be seen, although the effect of the temperature on the fluorescence intensity is similar in both proteins, the changes in the polarity and hydrophobicity around them were different from each other, and the N68F mutant decreased more significantly with the increasing temperature, and the T_m of it was almost lower than WT when the unfolding process monitored both by tryptophan fluorescence and tyrosine fluorescence. Under same denatured temperature, the difference of intrinsic fluorescence and ANS fluorescence showed that the loss of structure was larger in the N68F mutant than in the WT. So it can be concluded that thermal stability of the N68F mutant is inferior to WT, it may be anticipated that the N68 in apo-CP43 not only the potential binding sites of the pigment, but also the key amino acid stabilize the structure of transmembrane helix, so the N68 site mutagenesis decrease the thermostability of the apo-CP43. In summary, our results primarily suggest the motif around N68 in the transmembrane helices I of apo-CP43 play a important role in aggregation, and structural changes after heat treatment.

The results obtained were of some interest, and the reasons and meanings of this observation remain to be studied further to pursue more precise conclusions about the

stability of apo-CP43 and the mutants.

ACKNOWLEDGEMENT

The work was supported by the National Basic Research 973 Program 2009CB118502, the National Natural Sciences Foundation of China (No.30870181, 31170223) and the Doctoral Foundation of Ministry of Education of China (20070610168).

REFERENCES

- [1] T.J. Wydrzynski, K. Satoh, Photosystem: the light-driven water:plastoquinone oxidoreductase, Springer, The Netherlands, 2005.
- [2] A. Zouni, H.T. Witt, J. Kern, P. Fromme, N. Krauss, W. Saenger and P. Orth, Crystal structure of photosystem II from *Synechococcus elongatus* at 3.8 Å resolution, *Nature*. 409 (2001) 739–743.
- [3] K.N. Ferreira, T.M. Iverson, K. Maghlaoui, J. Barber and S. Iwata, Architecture of the photosynthetic oxygen-evolving center, *Science*. 303 (2004) 1831–1838.
- [4] A. Guskov, J. Kern, A. Gabdulkhakov, M. Broser, A. Zouni and W. Saenger, Cyanobacterial photosystem II at 2.9-Å resolution and the role of quinones, lipids, channels and chloride, *Nat. Struct. Mol. Biol.* 16 (2009) 334–342.
- [5] B. Loll, J. Kern, W. Saenger, A. Zouni, J. Biesiadka, Towards complete cofactor arrangement in the 3.0 Å resolution structure of photosystem II, *Nature* 438 (2005) 1040–1044.
- [6] N. Kamiya and J.R. Shen, Crystal structure of oxygen-evolving photosystem II from *Thermosynechococcus vulcanus* at 3.7-Å resolution, *Proc. Natl. Acad. Sci. USA* 100 (2003) 98–103.
- [7] Y. Umena, K. Kawakami, J.R. Shen and N. Kamiya, Crystal structure of oxygen-evolving photosystem II at a resolution of 1.9 Å. *Nature* 473 (2011) 55–60.
- [8] T.M. Bricker and L.K. Frankel, The structure and function of CP47 and CP43 in photosystem II, *Photosynth. Res.* 72 (2002) 131–146.
- [9] J. Barber, E. Morris and C. Büchel, Revealing the structure of the photosystem II chlorophyll binding proteins, CP43 and CP47, *Biochim. Biophys. Acta.* 1459 (2000) 239–247.
- [10] F. Müh, T. Renger and A. Zouni, Crystal structure of cyanobacterial photosystem II at 3.0 Å resolution: A closer look at the antenna system and the small membrane-intrinsic subunits, *Plant Physiol. Biochem.* 46 (2008) 238–264.
- [11] W.F.J. Vermaas, M. Ikeuchi and Y. Inoue, Protein composition of the Photosystem II core complex in genetically engineered mutants of the cyanobacterium *Synechocystis* PCC 6803, *Photosynth. Res.* 17 (1988) 97–113.
- [12] J.D. Rochaix, M. Kuchka, S. Mayfield, M. Schirmer-Rahire, B.J. Girard and P. Bennoun, Nuclear and chloroplast mutations affect the synthesis or stability of the chloroplast psbC gene product in *Chlamydomonas reinhardtii*, *EMBO J.* 8 (1989) 1013–1021.
- [13] M.G. Kuhn and W.F.J. Vermaas, Deletion mutations in a long hydrophilic loop in the photosystem II chlorophyll-binding protein CP43 in the cyanobacterium *Synechocystis*

- sp. PCC 6803, *Plant Mol. Biol.* 23 (1993) 123–133.
- [14] N. Knoepfle, T.M. Bricker and E.C. Putnam, Site-directed mutagenesis of basic arginine residues 305 and 342 in the CP43 protein of Photosystem II affects oxygen-evolving activity in *Synechocystis* 6803, *Biochemistry* 38 (1999) 1582–1588.
- [15] C. Rosenberg, J. Christian, T.M. Bricker and E.C. Putnam, Site-directed mutagenesis of glutamate residues in the large extrinsic loop of the photosystem II protein CP 43 affects oxygen-evolving activity and PS II assembly, *Biochemi.* 38 (1999) 15994–16000.
- [16] P. Manna and W. Vermaas, Mutational studies on conserved histidine residues in the chlorophyll-binding protein CP43 of photosystem II, *Eur. J. Biochem.* 247 (1997) 666–672.
- [17] R.J. Falconer, M. Marangon, S.C. Van Sluyter, K.A. Neilson, C. Chan, E.J. Waters and J. Agric, Thermal stability of thaumatin-like protein, Chitinase, and Invertase isolated from *Sauvignon blanc* and *Semillon Juice* and their role in haze formation in wine, *Food Chem.* 58 (2010) 975–980.
- [18] R.S. Sai Kumar, S.A. Singh and A.G. Rao, Conformational stability of α -amylase from malted sorghum (*Sorghum bicolor*): Reversible unfolding by denaturants, *Biochimie.* 91 (2009) 548–557.
- [19] X. Wu, M. Oppermann, K.D. Berndt, T. Bergman, H. Jornvall, S. Knapp and U. Oppermann, Thermal unfolding of the archaeal DNA and RNA binding protein Ssh10, *Biochem. Biophys. Res. Commun.* 373 (2008) 482–487.
- [20] S. Ebbinghaus, A. Dhar, J.D. McDonald and M. Gruebele, Protein folding stability and dynamics imaged in a living cell, *Nat. Methods* 7 (2010) 319–323.
- [21] A.N. Bullock, J. Henckel and A.R. Fersht, Quantitative analysis of residual folding and DNA binding in mutant p53 core domain: definition mutant states for rescue in cancer therapy, *Oncogene* 19 (2000) 1245–1256.
- [22] L. Stryer, Fluorescence spectroscopy of proteins (Fluorescence spectroscopy of proteins, analyzing polarity, distances between groups, flexibility and conformational transitions), *Science.* 162 (1968) 526–533.
- [23] F. Ding, W. Liu, X. Zhang, L.J. Wu, L. Zhang and Y. Sun, Identification of pyrazosulfuron-ethyl binding affinity and binding site subdomain IIA in human serum albumin by spectroscopic methods, *Spectrochim. Acta A Mol. Biomol. Spectrosc.* 75 (2010) 1088–1094.
- [24] S.S. Xie, J. Liu, J.Z. Wang, G.F. Zhu and L.F. Du, Unfolding of apo-CP43 induced by guanidine hydrochloride, *Chin. J. Appl. Environ. Biol.* 18 (2012) 373–377.
- [25] W.C. Albert, W.M. Gregory and G.S. Allan, The binding interaction of coomassie blue with Protein, *Biochem.* 213 (1993) 407–413.
- [26] T. Yamamoto, N. Fukui, A. Hori and Y. Matsui, Circular dichroism and fluorescence spectroscopy studies of the effect of cyclodextrins on the thermal stability of chicken egg white lysozyme in aqueous solution, *J. Mol. Struct.* 782 (2006) 60–66.
- [27] C.N. Pace, Determination and analysis of urea and guanidine hydrochloride denaturation curves, *Method. Enzymol.* 131 (1986) 266–280.
- [28] S. Paul, M. Kundu, K.P. Das, S. Mishra and T.K. Chaudhuri, Unfolding studies of *Escherichia coli* maltodextrin glucosidase monitored by fluorescence spectroscopy, *J. Biol. Phys.* 34 (2008) 539–550.

- [29] H.Q. Li, X.Y. Zheng, E.G. Pang, Y.Q. Zhao and B.S. Yang, The effect of Trp83 mutant on the properties of CopC, *Spectrochim. Acta Part A*. 70 (2008) 384–388.
- [30] C. Asima and B. Soumen, Interaction with Al and Zn induces structure formation and aggregation in natively unfolded caseins, *J. Photochem. Photobiol. B: Biol.* 93 (2008) 36–43.
- [31] M. Masomeh, G. Sirous and K. Reza, Spectroscopic study on the interaction of celecoxib with human carbonic anhydrase II: Thermodynamic characterization of the binding process, *J. Photochem. Photobiol. B: Biol.* 97 (2009) 161–168.
- [32] D. Samuel, T.K.S. Kumar, T. Srimathi, H.C. Hsieh and C. Yu, Identification and characterization of an equilibrium intermediate in the unfolding pathway of an all β -Barrel protein, *J. Biol. Chem.* 275 (2000) 34968–34975.
- [33] J.R. Lakowicz, *Principles of Fluorescence Spectroscopy*, Plenum Press. 3 (2006) 954.
- [34] J. Yang, Z.H. Jing, J.J. Jie and P. Guo, Fluorescence spectroscopy study on the interaction between Gossypol and bovine serum albumin, *J. Mol. Struct.* 920 (2009) 227–230.
- [35] H. Shi, L. Xiong, K.Y. Yang, C.Q. Tang, T.Y. Kuang and N.M. Zhao, Protein secondary structure and conformational changes of photosystem II during heat denaturation studied by Fourier transform-infrared spectroscopy, *J. Mol. Struct.* 446 (1998) 137–147.
- [36] J. De Las Rivas and J. Barber, Structure and thermal stability of photosystem II reaction centers studied by infrared spectroscopy, *Biochemi.* 36 (1997) 8897–8903.
- [37] J.S. Wang, J.X. Shan, Q. Xu, X. Ruan, Y.D. Gong, T.Y. Kuang and N.M. Zhao, Light-and heat-induced denaturation of photosystem II core-antenna complexes CP43 and CP47, *J. Photochem. Photobiol. B: Biol.* 50 (1999) 189-196.
- [38] Y.G. Qu, H. Chen, X.C. Qin, L.B. Li, L. Wang and T.Y. Kuang, Thermal denaturation of CP43 studied by Fourier transform-infrared spectroscopy and terahertz time-domain spectroscopy, *Biochim. Biophys. Acta.* 1774 (2007) 1614–1618.
- [39] D. Matulis and R. Lovrien, 1-Anilino-8-naphthalene sulfonate anion-protein binding depends primarily on ion pair formation, *Biophys. J.* 74 (1998) 422–429.
- [40] F. Ding, G.Y. Zhao, S.C. Chen, F. Liu, Y. Sun and L. Zhang, Chloramphenicol binding to human serum albumin: Determination of binding constants and binding sites by steady-state fluorescence, *J. Mol. Struct.* 929 (2009) 159–166.